PERGAMON

International Journal of Heat and Mass Transfer 46 (2003) 731–747

International Journal of HEAT and MASS TRANSFER

www.elsevier.com/locate/ijhmt

Transient coupled heat transfer in multilayer composite with one specular boundary coated

He-Ping Tan, Jian-Feng Luo *, Xin-Lin Xia, Qi-Zheng Yu

School of Energy Science and Engineering, Harbin Institute of Technology, Harbin 150001, China

Received 21 June 2002

Abstract

By the ray tracing\node method, the transient coupled radiative and conductive heat transfer in absorbing, scattering multilayer composite is investigated with one surface of the composite being opaque and specular, and the others being semitransparent and specular. The effect of Fresnel's reflective law and Snell's refractive law on coupled heat transfer are analyzed. By using ray tracing method in combination with Hottel and Sarofim's zonal method and spectral band model, the radiative intensity transfer model have been put forward. The difficulty for integration to solve radiative transfer coefficients (RTCs) is overcame by arranging critical angles according to their magnitudes. The RTCs are used to calculated radiative heat source term, and the transient energy equation is discretized by control volume method. The study shows that, for intensive scattering medium, if the refractive indexes are arranged decreasingly from the inner part of the composite to both side directions respectively, then, the total reflection phenomenon in the composite is advantageous for the scattered energy to be absorbed by the layer with the biggest refractive index, so at transient beginning a maximum temperature peak may appear in the layer with the biggest refractive index.

Keywords: Transient coupled radiative and conductive heat transfer; Multi-layer composite; Opaque or semitransparent; Ray freezing; Radiative transfer coefficient

1. Introduction

Semitransparent material has broad applications in industry, such as the insulating technology for the protection of aeroengine and turbine blade [1,2], the ignition and flame spread of semitransparent solid [3,4], the manufacture of glass and its application in high temperature environment [5,6], the silica insulation for the use of solar energy [7,8], the melting and removal of ice layer, the processing of multilayer semiconductors, and so on.

For semitransparent materials, refractive index takes very important role in their radiative heat transfer because the reflection at an interface is affected by the refractive indexes of the media on both sides of the interfaces, and also, the emitting ability of medium is in proportion to the square of refractive index. Siegel has taken a very deep investigation on the effect of refractive index on radiative heat transfer in semitransparent medium [9–12]. As discussed by Siegel, the diffuse reflectivity of interface can be obtained by integrating over the whole hemispherical space for the reflected energy if assuming each rough bit can acts as an optical smooth facet so that Fresnel's reflective law and Snell's refractive law can applied to each facet. The diffuse reflectivity is not angularly dependent and the total reflection effect is considered in the reflectivity formula.

However for semitransparent and specular interface, the specular reflectivity is angularly dependent and directly determined by Fresnel's reflective law and Snell's refractive law, and total reflection occurs when the incident angle is

* Corresponding author.
E-mail addresses: luo_jianfeng@yahoo.com (J.-F. Luo), xinlin_xia@sohu.com (X.-L. Xia).

0017-9310/03/$ - see front matter
PII: S0017-9310(02)00322-8

Nomenclature

A_{k,T_i}	fractional spectral emissive power of spectral band k at nodal temperature T_i, $\int_{\Delta\lambda_k} I_{\lambda,b}(T_i)\mathrm{d}\lambda/(\sigma T_i^4)$
$a1,a2$	surface, interface or control volume, used to define one-layer radiative intensity quotient transfer function
$b1,b2$	surface or interface, used to define multi-layer radiative intensity quotient transfer function
c_b	specific heat capacity of bth layer, $\mathrm{J\,kg^{-1}\,K^{-1}}$
E_n	exponential integral functions, $E_n(x)=\int_0^1 \mu^{n-2}\exp(-x/\mu)\,\mathrm{d}\mu$
F	radiative intensity quotient transfer function of one-layer STM model
H	radiative intensity quotient transfer function of multi-layer STM model
I_b	Ith node in bth layer
h_1, h_2	convective heat transfer coefficients at surfaces S_1 and S_2 respectively, $\mathrm{W\,m^{-2}\,K^{-1}}$
k_b	thermal conductivity of bth layer of medium, $\mathrm{W\,m^{-1}\,K^{-1}}$
k_{ie}, k_{iw}	harmonic mean thermal conductivity at interface ie and iw, $\mathrm{W\,m^{-1}\,K^{-1}}$
L_b	thickness of bth layer, m
L_t	total thickness of composite, $L_1+L_2+\cdots+L_n$, m
M_b	number of control volumes of bth layer
M_t	total number of control volumes of composite, $M_1+M_2+\cdots+M_n$
n	total number of layers of multi-layer composite
$n_{b,k}$	spectral refractive index of bth layer
$n'_{i,k}$	refractive index of ith control volume; when $i\leqslant M_1$, $n'_{i,k}=n_{1,k}$; when $M_1+M_2+\cdots+M_{b-1}<i\leqslant M_1+M_2+\cdots+M_b$, $n'_{i,k}=n_{b,k}$
n_0,n_{n+1}	refractive indexes of the surroundings (equal to the refractive index of air n_g)
N_b	conduction–radiation parameter of bth layer, $k_b/(4\sigma T_r^3 L_t)$
NB	total number of spectral bands
$P_b,P_{b'}$	interface between bth layer and $(b+1)$th layer, facing towards bth layer or $(b+1)$th layer, respectively
q^c,q^r,q^{cv}	thermal conductive, radiative and convective heat fluxes, respectively, $\mathrm{W\,m^{-2}}$
q^t	total heat flux, q^c+q^r, $\mathrm{W\,m^{-2}}$
$\tilde{q}$	dimensionless heat flux, $q/(\sigma T_r^4)$
RTC	radiative transfer coefficient
$S_{-\infty},S_{+\infty}$	left and right black surfaces representing the surroundings (Fig. 1)
S_1,S_2	boundary surfaces
S_u,S_v	surfaces for u, $v=1$, or 2
STM	semitransparent medium
T	absolute temperature, K
T_0	uniform initial temperature, K
T_r	reference temperature, K
T_{g1},T_{g2}	gas temperature for convection at $x=0$ and L_t, respectively, K
T_{S_1},T_{S_2}	gas temperatures for convection at $x=0$ and L_t, respectively, K
$T_{-\infty},T_{+\infty}$	temperatures of the black surface $S_{-\infty}$ and $S_{+\infty}$ respectively, K
t	physical time, s
t^*	dimensionless time, $t4\sigma T_r^3/(\rho_1 c_1 L_t)$
V_i	ith control volume, $i=1\sim M_t$
V_{I_b}	Ith control volume of bth layer, $I=1\sim M_b$
$(V_iV_j)_k,[V_iV_j]_k$	parts of radiative energy emitted by V_i at the kth spectral band $(\Delta\lambda_k)$ and absorbed by V_j for non-scattering and scattering media, respectively
$(S_uS_v)_k,[S_uS_v]_k$	parts of radiative energy emitted by S_u at the kth spectral band $(\Delta\lambda_k)$ and absorbed by S_v for non-scattering and scattering media, respectively
$(S_uV_j)_k,[S_uV_j]_k$	parts of radiative energy emitted by S_u at the kth spectral band $(\Delta\lambda_k)$ and absorbed by V_j for non-scattering and scattering media, respectively
$(V_iS_v)_k,[V_iS_v]_k$	parts of radiative energy emitted by V_i at the kth spectral band $(\Delta\lambda_k)$ and absorbed by S_v for non-scattering and scattering media, respectively
x	coordinate in direction across layer, m
x_i,y_i	geometrical progressions used in tracing radiative intensity's transferring

x_a^b distance between surface a and b, m
X dimensionless coordinate in direction across layer, $X = x/L_t$

Greek symbols

$\alpha_{b,k}$ spectral absorbing coefficient of bth layer, m^{-1}
β common ratio of geometric progression
Γ attenuated quotient of radiative intensity by control volume or surface
$\gamma(\theta)_{bo}$ transmissivity of radiative intensity propagating from layer "b" to layer "o" at angle θ, $\gamma(\theta)_{bo} = 1 - \rho(\theta)_{bo}$
Δx_b control volume thickness of bth layer, m
Δt time step, s
Δt^* dimensionless time step
$(\delta x)_{ie}$, $(\delta x)_{iw}$ distance between nodes i and $(i+1)$, and that between nodes i and $(i-1)$, respectively, m
$\varepsilon_{i,k}$, $\varepsilon_{o,k}$ emissivities of the inside and outside of surface S_2
$\varepsilon_{-\infty,k}$, $\varepsilon_{+\infty,k}$ emissivities of the black surfaces $S_{-\infty}$ and $S_{+\infty}$ respectively
η_b $1 - \omega_b$
η'_i $1 - \omega'_i$
Θ dimensionless temperature, T/T_r
θ incidence angle, rad
θ_{ij} critical angle, $\arcsin(n_j/n_i)$, if $n_i > n_j$
$\kappa_{b,k}$ extinction coefficients of bth layer, $\alpha_{b,k} + \sigma_{s,b,k}$, m^{-1}
λ wavelength, μm
ρ_b density of bth layer, $kg\,m^{-3}$
$\rho(\theta)_{bo}$ reflectivity of intensity going from layer "b" to layer "o" at angle θ
σ Stefan–Boltzman constant, $W\,m^{-2}\,K^{-4}$
$\sigma_{s,b,k}$ spectral scattering coefficient of bth layer, m^{-1}
$\tau_{b,k}$ spectral optical thickness of bth layer, $\kappa_{b,k}L_b$
Φ_i^r radiative heat source of control-volume i
$\omega_{b,k}$ spectral scattering albedo of bth layer, $\sigma_{s,b,k}/\kappa_{b,k}$
$\omega'_{i,k}$ spectral scattering albedo of ith control volume; when $i \leqslant M_1$, $\omega'_{i,k} = \omega_{1,k}$; when $M_1 + M_2 + \cdots + M_{b-1} < i \leqslant M_1 + M_2 + \cdots + M_b$, $\omega'_{i,k} = \omega_{b,k}$

Superscripts

m time step
s specular reflection
$*$ normalized values

Subscripts

a, b, c layer index, $a, b = (1 \sim n)$, c
bo from layer "b" to layer "o"
g gas (air)
i, j relative to node i to j
ie, iw right and left interfaces of control volume i
k relative to spectral band k
o oth layer, either $b-1$ or $b+l$ layer
t − o refers to a composite with semitransparent S_1 and opaque S_2
S_1, S_2 relative to surface S_1 or S_2
va relative to vacuum space
$-\infty$, $+\infty$ relative to $S_{-\infty}$ and $S_{+\infty}$
$\|$, $\perp$ relative to component for parallel and perpendicular polarization, respectively

greater than critical angle. Siegel [10] investigated the effect of Fresnel's specular reflective boundary on radiative heat transfer in an isothermal layer, and the unpolarized radiative incidence was divided into two equal, parallel and perpendicular components, which were traced separately. Liu and Dougherty [13] investigated the effect of Fresnel's

specular reflection on one-dimension radiative heat transfer in a semiinfinite anisotropic scattering medium, using variational technique to solve radiative transfer equation, Abulwafa [14] studied coupled radiative and conductive heat transfer in a linear anisotropic scattering plane-parallel medium, and considered the effect of semitransparent and specular boundary on heat transfer. Su and Sutton [15] investigated transient coupled heat transfer in an electric–magnetic window with refractive index being functions of wavelength and temperature, and the specular reflectivities of the surfaces are determined by Fresnel's reflective law and Snell's refractive law. By the ray tracing method, Tan and Lallemand [16] also investigated the effect of Fresnel's reflective law on transient coupled heat transfer in a one-layer medium.

As layer number increases, the total reflection at the semitransparent and specular interfaces of the composite is intensively affected by the relative magnitude of refractive indexes of all the layers and becomes very complex. However this problem has been successfully solved by the ray tracing method [17,18], and the transient coupled heat transfer in a multilayer composite is further investigated with semitransparent specular interfaces and semitransparent specular surfaces [19] or opaque specular surfaces [20]. In this paper, the multilayer composite is extended to as one boundary is semitransparent specular and the other is opaque specular, all of the interfaces of the composite are semitransparent and specular, and the specular reflectivities of all the semitransparent interfaces and surface are determines by Fresnel's reflective law and Snell's refractive law, the boundary conditions on the surfaces are different from those of Refs. [19,20] due to existence of conduction and convection equilibrium, on the semitransparent surface or complexity of conduction, convection and radiation equilibrium for the the opaque surface.

Few papers investigated transient coupled radiative and conductive heat transfer in a multilayer composite. While as early as in 1986, Tsai and Nixon [21] and Timoshenko and Trenev [22] have already studied this problem. In Ref. [21] the interfaces of the composite is opaque, so the layers cannot exchange radiative energy directly because of the obstruction of opaque interface to radiation. The interfaces of the composite of Ref. [22] are formed by thin coatings, which not only absorb and reflect radiation, but also, transmit radiation in an isotropic manner. The Fresnel's reflective law and Snell's refractive law are not used to determine reflectivities of all the interfaces in both of the two papers. Siegel and Spuckler [11] investigated the effect of refractive index on radiative heat transfer in a multilayer composite with semitransparent and diffuse surfaces and interfaces.

2. Physical model and discrete governing equation

As shown in Fig. 1, a n-layer absorbing, isotropically scattering semitransparent composite is located between two black surfaces $S_{-\infty}$ and $S_{+\infty}$, which denote the surroundings outside the two boundary surfaces S_1 and S_2, respectively. The surface S_1 is semitransparent and specular, while the surface S_2 is opaque (with coating) and specular, and all of the interfaces, $P_1, P_2, \ldots, P_{n-1}$, are semitransparent and specular. The optical and thermal physical properties of each layer of medium are different from each another. Along the thickness, the n layers are divided into M_1, $M_2, \ldots$, and M_n control volumes (inner nodes) respectively, and I_b is used to denote the Ith node in the bth layer, and for convenience,

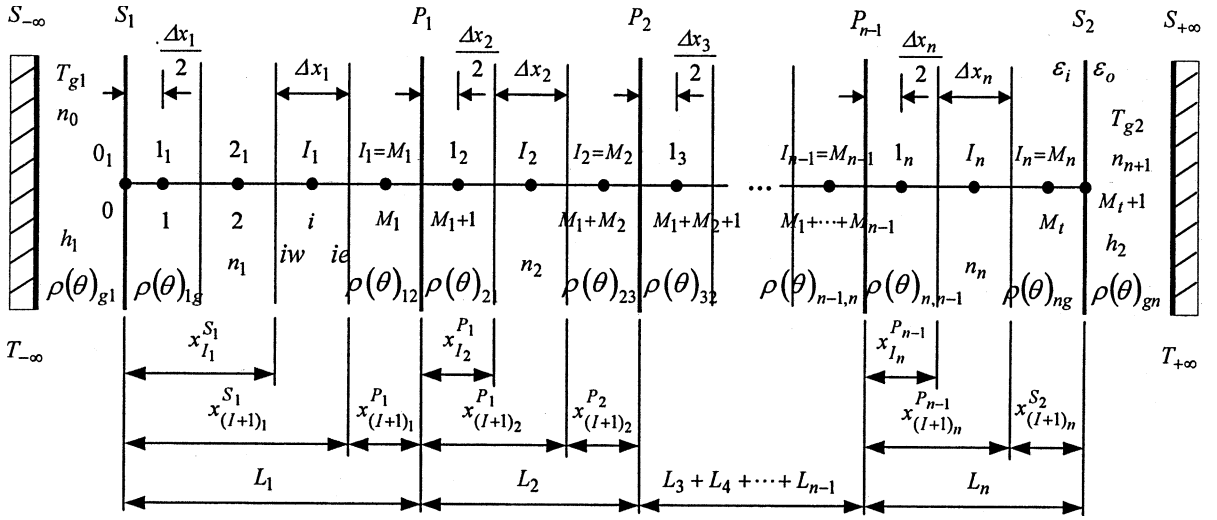

Fig. 1. Physical model of a n-layer semitransparent composite with one opaque specular surface.

all nodes are also denoted by i increasingly along the whole thickness. Let $M_t = M_1 + M_2 + \cdots + M_n$, then the total node number is $M_t + 2$ $(0, 1, \ldots, M_t + 1)$ with node 0 denoting S_1 and node $M_t + 1$ denoting S_2. $I_b = i$ if $b = 1$, and else $i = M_1 + M_2 + \cdots + M_{b-1} + I_b$.

The variation of the medium spectral properties with wavelength, such as κ_b, α_b, $\sigma_{s,b}$, and n_b etc., can be approximately expressed by a series of rectangular spectral bands. Thus, the fully implicit discrete energy equation of the ith control volume in the bth layer is [17,18]

$$\rho_b c_b \Delta x_b \frac{T_i^{m+1} - T_i^m}{\Delta t} = \frac{k_{ie}^{m+1}(T_{i+1}^{m+1} - T_i^{m+1})}{(\delta x)_{ie}} - \frac{k_{iw}^{m+1}(T_i^{m+1} - T_{i-1}^{m+1})}{(\delta x)_{iw}} + \Phi_i^{r,m+1} \tag{1}$$

The heat source term Φ_i^r of the ith control volume in Eq. (1) can be written for $1 \leqslant i \leqslant M_t$ as

$$\begin{aligned}\Phi_i^r = \sigma \sum_{k=1}^{\mathrm{NB}} \Bigg\{ \sum_{j=1}^{M_t} \Big\{ n_{j,k}'^2 [V_j V_i]_{k,\mathrm{t-o}}^{\mathrm{s}} A_{k,T_j} T_j^4 - n_{i,k}'^2 [V_i V_j]_{k,\mathrm{t-o}}^{\mathrm{s}} A_{k,T_i} T_i^4 \Big\} + \Big\{ n_{n,k}'^2 [S_2 V_i]_{k,\mathrm{t-o}}^{\mathrm{s}} A_{k,T_{S_2}} T_{S_2}^4 - n_{i,k}'^2 [V_i S_2]_{k,\mathrm{t-o}}^{\mathrm{s}} A_{k,T_i} T_i^4 \Big\} \\ + \Big\{ [S_{-\infty} V_i]_{k,\mathrm{t-o}}^{\mathrm{s}} A_{k,T_{-\infty}} T_{-\infty}^4 - n_{i,k}'^2 [V_i S_{-\infty}]_{k,\mathrm{t-o}}^{\mathrm{s}} A_{k,T_i} T_i^4 \Big\} \Bigg\}\end{aligned} \tag{2}$$

where subscript k denotes the kth spectral band. When $i = M_t + 1$, the radiative heat flux at surface S_2 is

$$q_{S_2}^r = \sigma \sum_{k=1}^{\mathrm{NB}} \Bigg\{ \sum_{j=1}^{M_t} \Big\{ n_{j,k}'^2 [V_j S_2]_{k,\mathrm{t-o}}^{\mathrm{s}} A_{k,T_j} T_j^4 - n_{n,k}'^2 [S_2 V_j]_{k,\mathrm{t-o}}^{\mathrm{s}} A_{k,T_{S_2}} T_{S_2}^4 \Big\} + [S_{-\infty} S_2]_{k,\mathrm{t-o}}^{\mathrm{s}} A_{k,T_{-\infty}} T_{-\infty}^4 - n_{n,k}'^2 [S_2 S_{-\infty}]_{k,\mathrm{t-o}}^{\mathrm{s}} A_{k,T_{S_2}} T_{S_2}^4 \Bigg\} \tag{3}$$

The boundary conditions are at surface S_1

$$2k_1(T_1 - T_{S_1})/\Delta x_1 = h_1(T_{S_1} - T_{\mathrm{g1}}) \tag{4a}$$

And that at surface S_2 is

$$q_{S_2}^r + 2k_n(T_{M_t} - T_{S_2})/\Delta x_n = \sigma \sum_{k=1}^{\mathrm{NB}} \varepsilon_{\mathrm{o},k}(A_{k,T_{S_2}} T_{S_2}^4 - A_{k,T_{+\infty}} T_{+\infty}^4) + h_2(T_{S_2} - T_{\mathrm{g2}}) \tag{4b}$$

3. RTCs of *n*-layer composite

The radiation transfer process in semitransparent medium (STM) can be divided into two sub-processes [23]: (1) emitting–attenuating–reflecting sub-process, in which only emitting, attenuating and reflecting of medium are considered, and the radiative transfer coefficients (RTCs) are represented by $(S_u S_v)_{k,\mathrm{t-o}}^{\mathrm{s}}$, $(S_u V_i)_{k,\mathrm{t-o}}^{\mathrm{s}}$, $(V_i S_u)_{k,\mathrm{t-o}}^{\mathrm{s}}$ and $(V_i V_j)_{k,\mathrm{t-o}}^{\mathrm{s}}$; (2) absorbing–scattering sub-process. After considering the effect of isotropic scattering of medium, the RTCs are represented by $[S_u S_v]_{k,\mathrm{t-o}}^{\mathrm{s}}$, $[S_u V_i]_{k,\mathrm{t-o}}^{\mathrm{s}}$, $[V_i S_u]_{k,\mathrm{t-o}}^{\mathrm{s}}$ and $[V_i V_j]_{k,\mathrm{t-o}}^{\mathrm{s}}$.

All of the RTCs satisfy the following relationship for such a multilayer physical model [23]:

$$\begin{aligned}&(S_{-\infty} S_2)_{k,\mathrm{t-o}}^{\mathrm{s}} = n_{n,k}^2 (S_2 S_{-\infty})_{k,\mathrm{t-o}}^{\mathrm{s}}, \qquad (S_{-\infty} V_{I_b})_{k,\mathrm{t-o}}^{\mathrm{s}} = n_{b,k}^2 (V_{I_b} S_{-\infty})_{k,\mathrm{t-o}}^{\mathrm{s}} \\ &n_{n,k}^2 (S_2 V_{I_b})_{k,\mathrm{t-o}}^{\mathrm{s}} = n_{b,k}^2 (V_{I_b} S_2)_{k,\mathrm{t-o}}^{\mathrm{s}}, \qquad n_{a,k}^2 (V_{I_a} V_{I_b})_{k,\mathrm{t-o}}^{\mathrm{s}} = n_{b,k}^2 (V_{I_b} V_{I_a})_{k,\mathrm{t-o}}^{\mathrm{s}}\end{aligned} \tag{5}$$

where subscripts "a" and "b" denote the ath and the bth layer respectively, and $a, b = 1 \sim n$.

3.1. Multi-layer intensity transfer model for emitting–attenuating–reflecting sub-process

Multi-layer radiative intensity quotient transfer functions are used here to trace the radiative intensity transferring in multilayer composite. The two sides of an interface should be specified first. Let P_m be the interface between the mth and the $(m + 1)$th layers, facing towards the mth layer as P_m, and that facing towards the $(m + 1)$th layer is denoted by $P_{m'}$.

The one-layer radiative intensity quotient transfer functions, expressed as $\mathbf{F}_{a1_b,k}^{a2_b}$, are shown in Appendix A. Seeing Fig. 2, the multilayer radiative intensity quotient transfer functions are expressed by $\mathbf{H}_{b1,m+1\sim m+\Delta m,k}^{b2}$, which means the total quotient of the spectral radiative intensity attenuated by superscript $b2$ (represents $P_{m'}$, $P_{m+1'}$, $P_{m+\Delta m-1}$ or $P_{m+\Delta m}$) to that emitted by subscript $b1$ (represents $P_{m'}$, or $P_{m+\Delta m}$) at kth spectral band after "transferring once" within the

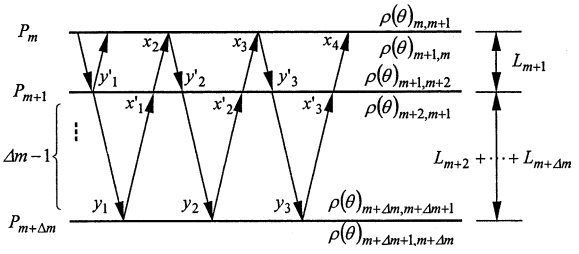

Fig. 2. Multi-layer radiative intensity transfer model.

multilayer model, where subscript $m+1 \sim m+\Delta m$ denotes the multilayer model is composed of from the $(m+1)$th to the $(m+\Delta m)$th layers. The "transferring once" means the process that the radiative intensity is attenuated and reflected repeatedly until it becomes 0 within the layers considered in the model. The quotient relates only to the layers from $(m+1)$th to the $(m+\Delta m)$th and the reflections at interface P_m, P_{m+1}, …, and $P_{m+\Delta m}$.

In the deduction of RTCs, as shown in Fig. 2, six multilayer radiative intensity quotient transfer functions are used: $\mathbf{H}^{P_{m'}}_{P_{m'},m+1\sim m+\Delta m,k}$, $\mathbf{H}^{P_{m+1'}}_{P_{m'},m+1\sim m+\Delta m,k}$, $\mathbf{H}^{P_{m+\Delta m}}_{P_{m'},m+1\sim m+\Delta m,k}$, $\mathbf{H}^{P_{m+\Delta m}}_{P_{m+\Delta m},m+1\sim m+\Delta m,k}$, $\mathbf{H}^{P_{m+\Delta m-1}}_{P_{m+\Delta m},m+1\sim m+\Delta m,k}$, and $\mathbf{H}^{P_{m'}}_{P_{m+\Delta m},m+1\sim m+\Delta m,k}$. Take the transferring process of the energy emitted by $P_{m'}$ is taken as an example to illustrate the deductive process of multilayer radiative intensity quotient transfer functions, subscript k is omitted.

(1) After "transferring once" within the $(m+1)$th layer, the quotient of radiative intensity arriving at P_{m+1} to that emitted by $P_{m'}$ for the first time is $y'_1 = \mathbf{F}^{P_{m+1}}_{P_{m'}}$.
(2) A fraction, $\gamma(\theta)_{m+1,m+2}$, of the above quotient that arrives at P_{m+1} enters the following $\Delta m-1$ layers, and after "transferring once" through the quotient arriving at $P_{m+1'}$ for the first time is $x'_1 = y'_1\gamma(\theta)_{m+1,m+2}\mathbf{H}^{P_{m+1'}}_{P_{m+1'},m+2\sim m+\Delta m}$. Only a part, $\gamma(\theta)_{m+2,m+1}$, of x'_1 enters the $(m+1)$th layer, and then after "transferring once" within this layer, the quotient arriving at P_{m+1} for the second time is $y'_2 = x'_1\gamma(\theta)_{m+2,m+1}\mathbf{F}^{P_{m+1}}_{P_{m+1}}$.
(3) The above quotient y'_2 repeats step (2), then the quotient arriving at P_{m+1} for the third time is $y'_3 = x'_2\gamma(\theta)_{m+2,m+1}\mathbf{F}^{P_{m+1}}_{P_{m+1}}$, where $x'_2 = y'_2\gamma(\theta)_{m+1,m+2}\mathbf{H}^{P_{m+1'}}_{P_{m+1'},m+2\sim m+\Delta m}$.
(4) Trace the radiative intensity by this way until it finally attenuates to 0. Then the total quotient arriving at P_{m+1} to that emitted by $P_{m'}$ is the sum of the infinite geometric series, $y'_1, y'_2, y'_3, \ldots$, with a common ratio of $\beta_2 = \gamma(\theta)_{m+2,m+1}\mathbf{F}^{P_{m+1}}_{P_{m+1}}\ \gamma(\theta)_{m+1,m+2}\mathbf{H}^{P_{m+1'}}_{P_{m+1'},m+2\sim m+\Delta m}(\beta_2 < 1)$. So there is:

$$\mathbf{H}^{P_{m+1}}_{P_{m'},m+1\sim m+\Delta m} = \sum_{i=1}^{\infty} y'_i = y'_1/(1-\beta_2) = \mathbf{F}^{P_{m+1}}_{P_{m'}}/(1-\beta_2) \tag{6}$$

(5) Based on Eq. (6) the multilayer radiative intensity quotient transfer functions, $\mathbf{H}^{P_{m+1'}}_{P_{m'},m+1\sim m+\Delta m}$ and $\mathbf{H}^{P_{m+\Delta m}}_{P_{m'},m+1\sim m+\Delta m}$ can be deduced as follows. Only a fraction, $\gamma(\theta)_{m+1,m+2}$, of the quotient $\mathbf{H}^{P_{m+1}}_{P_{m'},m+1\sim m+\Delta m}$ enters the following $\Delta m-1$ layers, and then:

$$\begin{aligned}\mathbf{H}^{P_{m+1'}}_{P_{m'},m+1\sim m+\Delta m} &= \sum_{i=1}^{\infty} x'_i = \mathbf{H}^{P_{m+1}}_{P_{m'},m+1\sim m+\Delta m}\gamma(\theta)_{m+1,m+2}\mathbf{H}^{P_{m+1'}}_{P_{m+1'},m+2\sim m+\Delta m} \\ &= \mathbf{F}^{P_{m+1}}_{P_{m'}}\gamma(\theta)_{m+1,m+2}\mathbf{H}^{P_{m+1'}}_{P_{m+1'},m+2\sim m+\Delta m}/(1-\beta_2)\end{aligned} \tag{7a}$$

$$\begin{aligned}\mathbf{H}^{P_{m+\Delta m}}_{P_{m'},m+1\sim m+\Delta m} &= \sum_{i=1}^{\infty} y_i = \mathbf{H}^{P_{m+1}}_{P_{m'},m+1\sim m+\Delta m}\gamma(\theta)_{m+1,m+2}\mathbf{H}^{P_{m+\Delta m}}_{P_{m+1'},m+2\sim m+\Delta m} \\ &= \mathbf{F}^{P_{m+1}}_{P_{m'}}\gamma(\theta)_{m+1,m+2}\mathbf{H}^{P_{m+\Delta m}}_{P_{m+1'},m+2\sim m+\Delta m}/(1-\beta_2)\end{aligned} \tag{7b}$$

Similarly, another quotient transfer function $\mathbf{H}^{P_{m'}}_{P_{m'},m+1\sim m+\Delta m,k}$ can be deduced as:

$$\mathbf{H}^{P_{m'}}_{P_{m'},m+1\sim m+\Delta m} = \sum_{i=1}^{\infty} x_i = \mathbf{F}^{P_{m'}}_{P_{m'}} + \mathbf{F}^{P_{m+1}}_{P_{m'}}\gamma(\theta)_{m+1,m+2}\mathbf{H}^{P_{m+1'}}_{P_{m+1'},m+2\sim m+\Delta m}\gamma(\theta)_{m+2,m+1}\mathbf{F}^{P_{m'}}_{P_{m+1}}/(1-\beta_2) \tag{7c}$$

As shown in Eqs. (7a)–(7c), $\mathbf{H}^{P_{m'}}_{P_{m'},m+1\sim m+\Delta m}$, $\mathbf{H}^{P_{m+\Delta m}}_{P_{m'},m+1\sim m+\Delta m}$ and $\mathbf{H}^{P_{m+\Delta m}}_{P_{m'},m+1\sim m+\Delta m}$ can be calculated from $\mathbf{H}^{P_{m+1'}}_{P_{m+1'},m+2\sim m+\Delta m}$ and $\mathbf{H}^{P_{m+\Delta m}}_{P_{m+1'},m+2\sim m+\Delta m}$, so Eqs. (7a)–(7c) is a recursive expression. Therefore, the calculation should be started from the

$(m+\Delta m)$th layer at first, i.e., $\mathbf{H}^{P_{m+\Delta m-1'}}_{P_{m+\Delta m-1'},m+\Delta m}=\mathbf{F}^{P_{m+\Delta m-1'}}_{P_{m+\Delta m-1'}}$ and $\mathbf{H}^{P_{m+\Delta m}}_{P_{m+\Delta m-1'},m+\Delta m}=\mathbf{F}^{P_{m+\Delta m}}_{P_{m+\Delta m-1'}}$. In combination with the one-layer radiative intensity quotient transfer functions $\mathbf{F}$ of the $(m+\Delta m-1)$th layer, the quotient $\mathbf{H}^{P_{m+\Delta m-2'}}_{P_{m+\Delta m-2'},m+\Delta m-1\sim m+\Delta m}$, $\mathbf{H}^{P_{m+\Delta m}}_{P_{m+\Delta m-2'},m+\Delta m-1\sim m+\Delta m}$ and $\mathbf{H}^{P_{m+\Delta m-1'}}_{P_{m+\Delta m-2'},m+\Delta m-1\sim m+\Delta m}$ can be calculated from Eqs. (7a)–(7c). Similarly, based on $\mathbf{H}^{P_{m+\Delta m-2'}}_{P_{m+\Delta m-2'},m+\Delta m-1\sim m+\Delta m}$and $\mathbf{H}^{P_{m+\Delta m}}_{P_{m+\Delta m-2'},m+\Delta m-1\sim m+\Delta m}$, and combining the one-layer radiative intensity quotient transfer functions, $\mathbf{F}$, of the $(m+\Delta m-2)$th layer, $\mathbf{H}^{P_{m+\Delta m-3'}}_{P_{m+\Delta m-3'},m+\Delta m-2\sim m+\Delta m}$, $\mathbf{H}^{P_{m+\Delta m}}_{P_{m+\Delta m-3'},m+\Delta m-2\sim m+\Delta m}$ and $\mathbf{H}^{P_{m+\Delta m-2'}}_{P_{m+\Delta m-3'},m+\Delta m-2\sim m+\Delta m}$ can be calculated from Eqs. (7a)–(7c). So, repeating the calculations, finally the quotient $\mathbf{H}^{P_{m'}}_{P_{m'},m+1\sim m+\Delta m}$, $\mathbf{H}^{P_{m+\Delta m}}_{P_{m'},m+1\sim m+\Delta m}$ and $\mathbf{H}^{P_{m+\Delta m}}_{P_{m'},m+1\sim m+\Delta m}$ can thus be calculated.

$\rho(\theta)$ and $\gamma(\theta)$ in Eqs. (7a)–(7c) are functions of polarized components, as shown in Appendix B, and so the value of Eqs. (7a)–(7c) differs in different component.

3.2. RTCs of multilayer composite for emitting–attenuating–reflecting sub-process

Resorting to the multilayer radiative intensity quotient transfer function, $\mathbf{H}$, the RTCs of n-layer absorbing-emitting composite ($\kappa_k=\alpha_k$) can be deduced conveniently. As shown in Eq. (5), there are seven categories of RTCs, and all of them must be deduced in the calculation. Take $(S_2V_{I_b})^{\mathrm{s}}_{k,\mathrm{t-o}}$ as an example to illustrate the deducing process of RTCs. For convenience, subscript k is omitted.

(1) As shown in Fig. 3, assume S_2 emits radiative intensity at spectral band k and at angle θ, then after "transferring once" within the layers the quotient of the radiative intensity arriving at $P_{b'}$, for the first time to that emitted by S_2 is $x_1=\mathbf{H}^{P'_b}_{S_2,b+1\sim n}$.

(2) A fraction, $\gamma(\theta)_{b+1,b}$, of the quotient that arrives at $P_{b'}$, will enter the upper layers from the first one to the bth one, a quotient, $\gamma(\theta)_{b+1,b}\mathbf{H}^{P_b}_{P_b,1\sim b}$, of the radiative intensity arrives at P_b, and then a part of the quotient will traverse P_b to enter the layers from the $(b+1)$th nth one, and after "transferring once" within these layers, the quotient of the radiative intensity arriving at $P_{b'}$ to that arriving at $P_{b'}$, will be $\gamma(\theta)_{b+1,b}\mathbf{H}^{P_b}_{P_b,1\sim b}\gamma(\theta)_{b,b+1}\mathbf{H}^{P_{b'}}_{P_{b'},b+1\sim n}$. So, the quotient of the radiative intensity arriving at $P_{b'}$, to that emitted by S_2 for the second time is $x_2=x_1\gamma(\theta)_{b+1,b}\mathbf{H}^{P_b}_{P_b,1\sim b}\gamma(\theta)_{b,b+1}\mathbf{H}^{P_{b'}}_{P_{b'},b+1\sim n}$.

(3) Quotient x_2 will repeat step (2), then the quotient of the radiative intensity arriving at $P_{b'}$, to that emitted by S_2 for the third time is $x_3=x_2\gamma(\theta)_{b+1,b}\mathbf{H}^{P_b}_{P_b,1\sim b}\gamma(\theta)_{b,b+1}\mathbf{H}^{P_{b'}}_{P_{b'},b+1\sim n}$.

(4) Tracing the transfer process again and again as the above does until the radiative intensity attenuates to zero within the n layers, then the total quotient arriving at $P_{b'}$ to that emitted by S_2 is the sum of the infinite geometric progression, $x_1,x_2,\ldots$, with a common ratio of $\beta_3=\gamma(\theta)_{b+1,b}\mathbf{H}^{P_b}_{P_b,1\sim b}\gamma(\theta)_{b,b+1}\mathbf{H}^{P_{b'}}_{P_{b'},b+1\sim n}$ $(\beta_3<1)$. So we can get:

$$\mathbf{H}^{P_{b'}}_{S_2,1\sim n}=\sum_{i=1}^{\infty}x_i=\mathbf{H}^{P_{b'}}_{S_2,b+1\sim n}/(1-\beta_3) \tag{8}$$

(5) Only a fraction, $\gamma(\theta)_{b+1,b}$, of the above quotient enters the bth layer, and the quotient of the radiative intensity received by V_{I_b}, to that emitted by S_2 after "transferring once" within the n layers and traversing P_b should be

$$\Gamma_1=\mathbf{H}^{P_{b'}}_{S_2,1\sim n}\gamma(\theta)_{b+1,b}\mathbf{F}^{V_{I_b}}_{P_b}=\mathbf{H}^{P_{b'}}_{S_2,b+1\sim n}\gamma(\theta)_{b+1,b}\mathbf{F}^{V_{I_b}}_{P_b}/(1-\beta_3) \tag{9}$$

The total quotient of the radiative intensity arriving at P_{b-1} to that emitted by S_2 after "transferring once" within the n layers can be deduced from Eq. (8), that is:

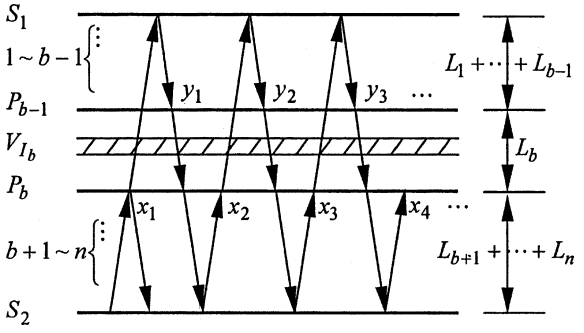

Fig. 3. Deduction of RTC $(S_2V_{I_b})^{S}_{k,\mathrm{t-o}}$.

$$\mathbf{H}_{S_2,1\sim n}^{P_{b-1}}=\sum_{i=1}^{\infty}y_i=\mathbf{H}_{S_2,1\sim n}^{P_{b'}}\gamma(\theta)_{b+1,b}\mathbf{H}_{P_b,1\sim b}^{P_{b-1}}=\mathbf{H}_{S_2,b+1\sim n}^{P_{b'}}\gamma(\theta)_{b+1,b}\mathbf{H}_{P_b,1\sim b}^{P_{b-1}}/(1-\beta_3) \tag{10}$$

Only a fraction, $\gamma(\theta)_{b-1,b}$, of the above quotient $\mathbf{H}_{S_2,1\sim n}^{P_{b-1}}$ traverses P_{b-1} to enter the bth layer, then the quotient of the radiative intensity received by V_{I_b}, to that emitted by S_2 after "transferring once" within the n layers is

$$\Gamma_2=\mathbf{H}_{S_2,1\sim n}^{P_{b-1}}\gamma(\theta)_{b-1,b}\mathbf{F}_{P_{b-1}}^{V_{I_b}}=\mathbf{H}_{S_2,b+1\sim n}^{P_{b'}}\gamma(\theta)_{b+1,b}\mathbf{H}_{P_b,1\sim b}^{P_{b-1}}\gamma(\theta)_{b-1,b}\mathbf{F}_{P_{b-1}}^{V_{I_b}}/(1-\beta_3) \tag{11}$$

Finally, the total quotient of the radiative intensity received by V_{I_b} to that emitted by S_2 after "transferring once" within the n layers and traversing P_b and P_{b-1} can be deduced as:

$$\Gamma=\Gamma_1+\Gamma_2 \tag{12}$$

However, some special cases must be specified for Eq. (12): (1) if $b=n$, then $\Gamma_1=\mathbf{F}_{S_2}^{V_{I_b}}$, else Γ_1 is calculated from Eq. (9); (2) if $b=1$, then $\Gamma_2=0$, else Γ_2 is calculated from Eq. (11).

For an unpolarized radiative incidence, the radiative intensity can be divided as two equal, parallel and perpendicular components, and trace them separately as does in Ref. [10]. So for an unpolarized radiative incidence, the final received quotient can be expressed as

$$(\Gamma_{\parallel}+\Gamma_{\perp})/2 \tag{13}$$

By integrating expression (13) over the hemispherical space, the RTC $(S_2V_{I_b})_{k,\mathrm{t-o}}^{S}$ can thus be solved.

In $\rho(\theta)$ and $\gamma(\theta)$ the above equations can be calculated from the formulae presented in Appendix B, and $\rho(\theta)$ will be 1 if total reflection occurs. So, due to the effect of the total reflection, Eq. (13) is not a continuous function over the whole hemispherical space, and it cannot be integrated directly over the whole hemispherical space. Hence, the following method is applied.

(1) Solve the critical angle θ'_{na} of S_2 vs. the ath layer. If $n_n>n_a(a=0\sim n)$, then $\theta'_{na}=\arcsin(n_a/n_n)$, else $\theta'_{na}=\pi/2$. Due to $a=0\sim n$, $n+1$ angles can be obtained: θ'_{n0}, θ'_{n1}, $\theta'_{n2},\ldots,$ and θ'_{nn} and θ'_{nn} must equal to $\pi/2$.
(2) Arrange these angles from small to big, and a new array can be obtained. Assume the new array to be: $(\theta_{n(-1)}=)0<\theta_{n0}\leqslant\theta_{n1}\leqslant\theta_{n2}\cdots\theta_{nn}$, where θ_{nn} must equal to $\pi/2$.

The whole hemispherical space is divided into $(n+1)$ intervals according to the arranged critical angle array: $[\theta_{n(-1)},\theta_{n0}]$, $[\theta_{n0},\theta_{n1}]$, $[\theta_{n1},\theta_{n2}],\ldots,$ and $[\theta_{n(n-1),\theta_{nn}}]$, and within each interval, Γ is a continuous function, so that by integrating Eq. (13) within each interval and adding those results, and simultaneously considering the inside emissivity of S_2, the RTC $(S_2V_{I_b})_{k,\mathrm{t-o}}^{S}$ can be solved as:

$$(S_2V_{I_b})_{k,\mathrm{t-o}}^{S}=\varepsilon_{\mathrm{i},k}\sum_{a=-1}^{n-1}\int_{\theta_{na}}^{\theta_{n(a+1)}}\left(\Gamma_{\parallel}+\Gamma_{\perp}\right)\cos\theta\sin\theta\,\mathrm{d}\theta \tag{14}$$

The other RTCs also can be solved by the similar way, they are not written out here.

3.3. RTCs of multilayer composite for absorbing–scattering sub-process

For an isotropically scattering composite ($\kappa_k=\alpha_k+\alpha_{s,k}$), the RTCs $[S_uS_v]_{k,\mathrm{t-o}}^{\mathrm{s}}$, $[S_uV_i]_{k,\mathrm{t-o}}^{\mathrm{s}}$, $[V_iS_u]_{k,\mathrm{t-o}}^{\mathrm{s}}$ and $[V_iV_j]_{k,\mathrm{t-o}}^{\mathrm{s}}$ can be calculated from the RTCs $(S_uS_v)_{k,\mathrm{t-o}}^{\mathrm{s}}$, $(S_uV_i)_{k,\mathrm{t-o}}^{\mathrm{s}}$, $[V_iS_u]_{k,\mathrm{t-o}}^{\mathrm{s}}$ and $(V_iV_j)_{k,\mathrm{t-o}}^{\mathrm{s}}$ [17], where the subscripts $u,v=-\infty$ or 2. Superscript s, subscript (t − o) and k are omitted in the following deduction, subscript a is introduced to denote the absorbing part of radiative energy.

Before beginning the following deducing process, the RTCs for emitting-attenuating-reflecting sub-process should be normalized first:

$$(V_iV_j)^*=(V_iV_j)/(4\kappa_{b,k}\Delta x_b)\quad V_i\in b\text{th layer} \tag{15a}$$

$$(V_iS_u)^*=(V_iS_u)/(4\kappa_{b,k}\Delta x_b)\quad V_i\in b\text{th layer} \tag{15b}$$

$$(S_uV_j)^*=(S_iV_j)/\varepsilon_{u,k} \tag{15c}$$

$$(S_uS_v)^*=(S_uS_v)/\varepsilon_{u,k} \tag{15d}$$

where the superscript '$*$' denotes the normalized values. Take $[V_iV_j]$, as an example for illustration.

(1) After considering, the first scattering event, a fraction, η_i, of $(V_iV_j)^*$ is absorbed by V_j, i.e. $[V_iV_j]_a^{*1st} = (V_iV_j)^*\eta_j$. The energy emitted by V_i will be scattered by all of the control volumes, and causes some of the radiative energy to be absorbed by V_j.

(2) After considering the second scattering event, the absorbed energy by V_j becomes $[V_iV_j]_a^{*2nd} = [V_iV_j]_a^{*1st} + \sum_{l_2=1}^{M_t}(V_iV_{l_2})^*\omega_{l_2}(V_{l_2})^*\eta_j$. In the second step, the scattered energy, $\sum_{l_2=1}^{M_t}(V_iV_{l_2})^*\omega_{l_2}$ will be scattered by all of the control volumes again, and causes another fraction of energy to be absorbed by V_j.

(3) After considering the third scattering event,

$$[V_iV_j]_a^{*3rd} = [V_iV_j]_a^{*2nd} + \sum_{l_2=1}^{M_t}(V_iV_{l_2})^*\omega_{l_2}\left[\sum_{l_3=1}^{M_t}(V_{l_2}V_{l_3})^*\omega_{l_3}(V_{l_3}V_j)^*\eta_j\right]$$

(4) To trace the scattered energy again and again in the similar way, the calculation can be finished if $1 - [V_iV_j]_a^{*nth} < 10^{-10}$ after considering the nth scattering event, where

$$[V_iV_j]_a^{*nth} = [V_iV_j]_a^{*(n-1)th} + \sum_{l_2=1}^{M_t}(V_iV_{l_2})^*\omega_{l_2} \times\left\{\sum_{l_3=1}^{M_t}(V_{l_2}V_{l_3})^*\omega_{l_3}\left\{\sum_{l_4=1}^{M_t}(V_{l_3}V_{l_4})^*\omega_{l_4}\cdots\left\{\sum_{l_{n-1}=1}^{M_t}(V_{l_{n-2}}V_{l_{n-1}})^*\omega_{l_{n-1}}\left[\sum_{l_{n-1}}^{M_t}(V_{l_{n-1}V_{l_n}})^*\omega_{l_n}(V_{l_n}V_j)^*\eta_j\right]\right\}\right\}\right\} \tag{16a}$$

Then the RTC $[V_iV_j]$ can be calculated from the reverse calculation $[V_iV_j] = 4\kappa_b\eta_b\Delta x_b[V_iV_j]_a^{*nth}$ ($V_i \in bth$ layer) since $\alpha_b = \kappa_b\eta_b$. The rest RTCs, $[S_uS_v]$, $[V_jS_u]$ and $[S_uV_i]$ can be deduced similarly, so after considering the nth scattering event, such that $[S_uS_v] = \varepsilon_u[S_uS_v]_a^{*nth}$, $[V_iS_u] = 4\kappa_b\eta_b\Delta x_b[V_iS_u]_a^{*nth}$ and $[S_uV_i] = \varepsilon_u[S_uV_i]_a^{*nth}$, respectively

$$[S_uS_v]_a^{*nth} = [S_uS_v]_a^{*(n-1)th} + \sum_{l_2=1}^{M_t}(S_uV_{l_2})^*\omega_{l_2} \times\left\{\sum_{l_3=1}^{M_t}(V_{l_2}V_{l_3})^*\omega_{l_3}\left\{\sum_{l_4=1}^{M_t}(V_{l_3}V_{l_4})^*\omega_{l_4}\cdots\left\{\sum_{l_{n-1}=1}^{M_t}(V_{l_{n-2}}V_{l_{n-1}})^*\omega_{l_{n-1}}\left[\sum_{l_{n-1}}^{M_t}(V_{l_{n-1}V_{l_n}})^*\omega_{l_n}(V_{l_n}S_v)^*\right]\right\}\right\}\right\} \tag{16b}$$

$$[V_iS_u]_a^{*nth} = [V_iS_u]_a^{*(n-1)th} + \sum_{l_2=1}^{M_t}(V_iV_{l_2})^*\omega_{l_2} \times\left\{\sum_{l_3=1}^{M_t}(V_{l_2}V_{l_3})^*\omega_{l_3}\left\{\sum_{l_4=1}^{M_t}(V_{l_3}V_{l_4})^*\omega_{l_4}\cdots\left\{\sum_{l_{n-1}=1}^{M_t}(V_{l_{n-2}}V_{l_{n-1}})^*\omega_{l_{n-1}}\left[\sum_{l_{n-1}}^{M_t}(V_{l_{n-1}V_{l_n}})^*\omega_{l_n}(V_{l_n}S_u)^*\right]\right\}\right\}\right\} \tag{16c}$$

$$[S_uV_j]_a^{*nth} = [S_uV_j]_a^{*(n-1)th} + \sum_{l_2=1}^{M_t}(S_uV_{l_2})^*\omega_{l_2} \times\left\{\sum_{l_3=1}^{M_t}(V_{l_2}V_{l_3})^*\omega_{l_3}\left\{\sum_{l_4=1}^{M_t}(V_{l_3}V_{l_4})^*\omega_{l_4}\cdots\left\{\sum_{l_{n-1}=1}^{M_t}(V_{l_{n-2}}V_{l_{n-1}})^*\omega_{l_{n-1}}\left[\sum_{l_{n-1}}^{M_t}(V_{l_{n-1}V_{l_n}})^*\omega_{l_n}(V_{l_n}V_j)^*\eta_j\right]\right\}\right\}\right\} \tag{16d}$$

3.4. Numerical method and validation of RTCs

As shown in Eq. (2), the radiative heat source term Φ_i^r is a non-linear function of the temperatures of all nodes, so it should be linearized at first [16]. Then solving the linearized equations by the tri-diagonal matrix algorithm gives the temperatures of all nodes. The numerical method adapted is the same as that used in [16–20].

The results of this paper cannot be compared with those of other published papers because the similar physical model of other paper cannot be found. So the correctness of this paper is mainly validated by Eq. (5) and the following equation:

$$\sum_{j=1}^{M_t}\left(V_iV_j\right)_{k,\mathrm{t-o}}^{\mathrm{s}} + \left(V_iS_{-\infty}\right)_{k,\mathrm{t-o}}^{\mathrm{s}} + \left(V_iS_2\right)_{k,\mathrm{t-o}}^{\mathrm{s}} = 4\kappa_{b,k}\Delta x_b \quad V_i \in b\text{th layer} \tag{17a}$$

$$(S_{-\infty}S_{-\infty})^{s}_{k,t-o} + \sum_{j=1}^{M_t} (S_{-\infty}V_j)^{s}_{k,t-o} + (S_{-\infty}S_2)^{s}_{k,t-o} = 1 \tag{17b}$$

$$(S_2S_{-\infty})^{s}_{k,t-o} + \sum_{j=1}^{M_t} (S_2V_j)^{s}_{k,t-o} + (S_2S_2)^{s}_{k,t-o} = \varepsilon_{i,k} \tag{17c}$$

4. Results and discussions

In the following the heat transfer in gray medium is analyzed. The thickness, specific heat capacity, conduction–radiation parameter and optical properties of each layer can be different from each other, the refractive index of each layer is typically chosen as different from each other.

4.1. Effect of convective coefficient and emissivity on coupled heat transfer

The effect of convective coefficient on coupled heat transfer in a five-layer composite is investigated in Fig. 4. The solid lines are for $h_1 = h_2 = 0\ \mathrm{W\,m^{-2}\,K^{-1}}$, the dashed lines are for $h_1 = h_2 = 10\ \mathrm{W\,m^{-2}\,K^{-1}}$, the dotted lines are for $h_1 = h_2 = 100\ \mathrm{W\,m^{-2}\,K^{-1}}$, and the dash-dot lines are for $h_1 = h_2 = \infty$. Except for convective coefficient, the other parameters are the same for each group curves. The refractive index of each layer is indicated in the figure, and the other parameters are $T_{-\infty} = 1300$ K, $T_{+\infty} = T_{g1} = T_{g2} = T_0 = 300$ K, $T_r = 1000$ K, $\omega_b = 0 (b = 1\text{–}5)$, $L_b = 0.005$ m, $\kappa_b = 50\ \mathrm{m^{-1}}$ $\rho_b c_b =$ constant, $N_b = 0.001$, and $\varepsilon_i = \varepsilon_0 = 0.8$.

As shown in Fig. 4, the increase in both convective coefficients intensifies convective cooling on both surfaces, so the temperature of the composite decreases. The radiative energy emitted by $S_{-\infty}$ can traverse S_1, to exchange with the composite directly due to S_1 being semitransparent, so the first layer absorbs most energy and has the highest temperature. The convective cooling effect of left environment on S_1 cause the temperatures of S_1 and its near media to decrease intensively, so that a maximum temperature appears in the first layer. As shown by solid lines, when the convective coefficients are zero, the temperature curves are perpendicular to S_1 and have zero temperature gradient at S_1, but at S_2 which is opaque, it can absorb and emit radiative energy, and the change of its temperature can affect the exchange of radiative energy among the media of the composite and the environment. So as shown in the Fig. 4, when both convective coefficients increase to cause the temperatures of both surfaces to be decreased, S_1 transfers energy to the inner part of the composite in conduction manner and affects slowly the temperature of the composite, so at transient beginning, such as at $t^* = 0.2$, all curves almost superpose with each other in the first layer; however, S_2 can promptly affect the temperature of the whole composite in radiation manner, that the temperatures of the layers from

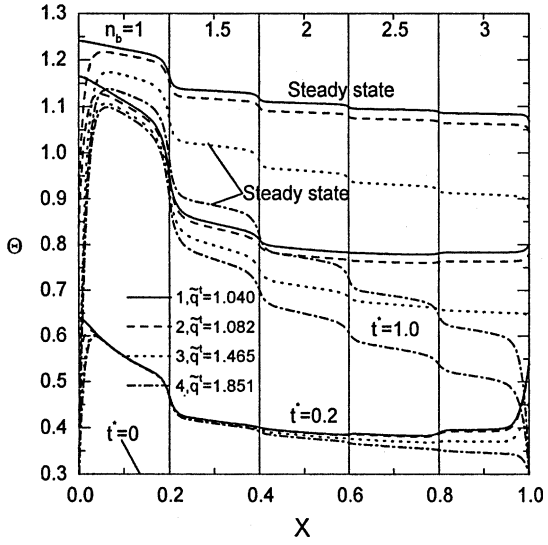

Fig. 4. Effect of convective coefficient on coupled heat transfer.

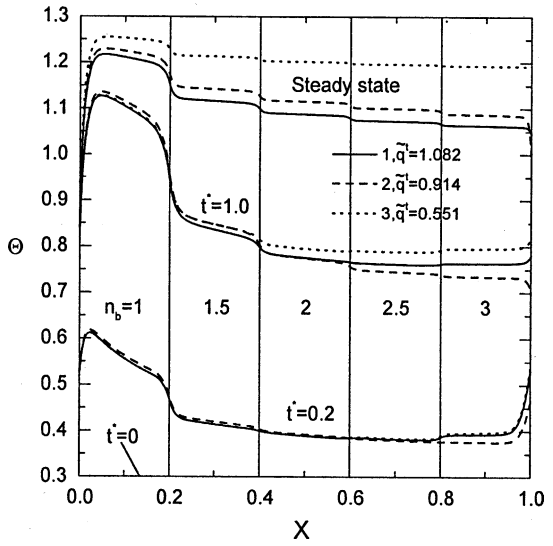

Fig. 5. Effect of emissivity on coupled heat transfer.

the second to the fifth decrease intensively. The absorbing effect inside of S_2 causes the surface S_2 transmit more convective energy to the fluid of external environment, so that the increase in convective coefficients can cause steady heat flux to increase, and the steady heat flux reaches a max value when $h_1 = h_2 = \infty$.

In Fig. 5, the calculating parameters of the solid lines are the same with those of the dashed lines in Fig. 4 with $\varepsilon_i = \varepsilon_0 = 0.8$, the emissivities on both sides of S_2 are changed. The results of $\varepsilon_i = 0.2$ and $\varepsilon_0 = 0.8$ are shown in dashed lines, and those of $\varepsilon_i = 0.8$ and $\varepsilon_0 = 0.2$ are shown in dotted lines. As shown in Fig. 5, when ε_i decreases, the absorption inside of S_2 is weakened, and the reflection therein is intensified, so the temperature of S_2 decreases, the steady temperature most of the composite increases, and the steady heat flux decreases. When ε_0 decreases, the radiative cooling ability of S_2 to $S_{-\infty}$ is weakened, so the temperature of S_2 increases, the steady state temperature of the composite are much higher than those of the other two curves, and the steady heat flux decreases also as shown in the figure. So the decrease in any of the emissivities of S_2 makes the heat transfer ability of the composite to be weakened, and the outside emissivity can cause bigger effect on heat transfer than that of the inside emissivity does.

4.2. Comparison of effects of radiative incidence on coupled heat transfer

Figs. 6 and 7 show the effects of refractive index and scattering albedo on coupled heat transfer when external radiative incidence on semitransparent surface and opaque surface, respectively. In both figures, the scattering albedo of solid lines is $\omega_b = 0 (b = 1–5)$, that of dashed lines is $\omega_b = 0.5$, and that of dotted lines is $\omega_b = 0.9$. The calculating parameters of the solid lines in Fig. 6(a), are the same with those of the dashed lines in Fig. 4, the other parameters of the dashed lines and the dotted lines are the same with those of solid lines except for scattering albedo. As scattering albedo increase to 0.9, the transient temperature distribution of the composite for the dotted lines increases from left to right, caused by total reflection. The total reflection occurs at the right side of each semitransparent interface if refractive indexes are arranged increasingly along the thickness. When the radiative energy emitted by $S_{-\infty}$ entens the composite from S_1, most of it is to be scattered, and if the incident angle of the scattered energy is greater than the critical angle, then, the scattered energy will be totally reflected. So the more the interfaces locates in the left side, the more the energy reflected by total reflection from the scattering energy, the higher the temperature of the layer is. Scattering makes the inside of S_2 absorbed more radiative energy, its temperature increases, the exchange of convection and radiation outside of S_2 with external environment is intensified thereby, and the steady heat flux increases.

Except for refractive index arrangement, the other parameters of Fig. 6b are the same with those of Fig. 6(a). For this condition total reflection occurs at the left side of each interface, so, as the scattering albedo increases to $\omega_b = 0.9$, the increasing temperature distribution along the thickness in Fig. 6(a) does not appear in Fig. 6(b) at transient beginning. The more intensively the medium of the composite scatters, the greater the steady heat flux is. As shown for $n_1 = 3$, makes the reflection of S_1 intensified, so less of the radiative energy emitted by $S_{-\infty}$ enters the composite from S_1, this causes the steady heat flux to be smaller than that of corresponding curve in Fig. 6(a).

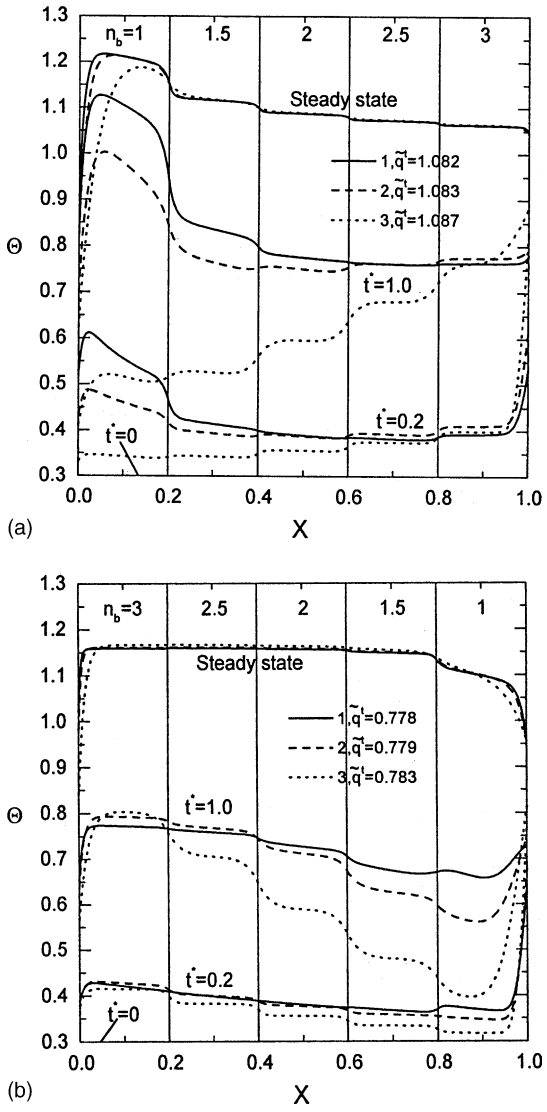

Fig. 6. Coupled heat transfer for radiative incidence on semitransparent surface. (a) Arranging refractive indexes increasingly along the thickness. (b) Arranging refractive indexes decreasingly along the thickness.

The temperature distributions for the case the environment incident radiative energy projected on opaque surface, with $T_{-\infty} = 300$ K and $T_{+\infty} = 1300$ K, are shown in Fig. 7(a) and (b), the other parameters are the same with those of corresponding curves in Fig. 6(a) and (b), respectively. Due to the resistance of opaque surface, the $S_{+\infty}$ can not directly exchange radiative energy with the inner part of the composite, but heats opaque surfaces first, and then transfers heat energy to the inner part of the composite by radiation and conduction. As shown in Fig. 7(a), the maximum temperature does not appear in the composite, the adding of isotropic scattering makes absorbing coefficient to be decreased, the emitting ability inside of S_2 is weakened, and the steady heat flux decreases, which is very different from those in Fig. 6(a).

Except for refractive index arrangement, the other parameters of Fig. 7(b) are the same with those of Fig. 7(a). Compared with Fig. 7(a), the temperature of S_2 rise more quickly and higher, but the temperatures of the layers from the first to the fourth rise slowly, and the steady heat fluxes decrease. The main reason is that the refractive index of the fifth layer ($n_5 = 1$) is much small and the emitting ability inside of S_2 becomes weak. Compared with Fig. 6(b), the heat flux of the corresponding curve of this figure decreases.

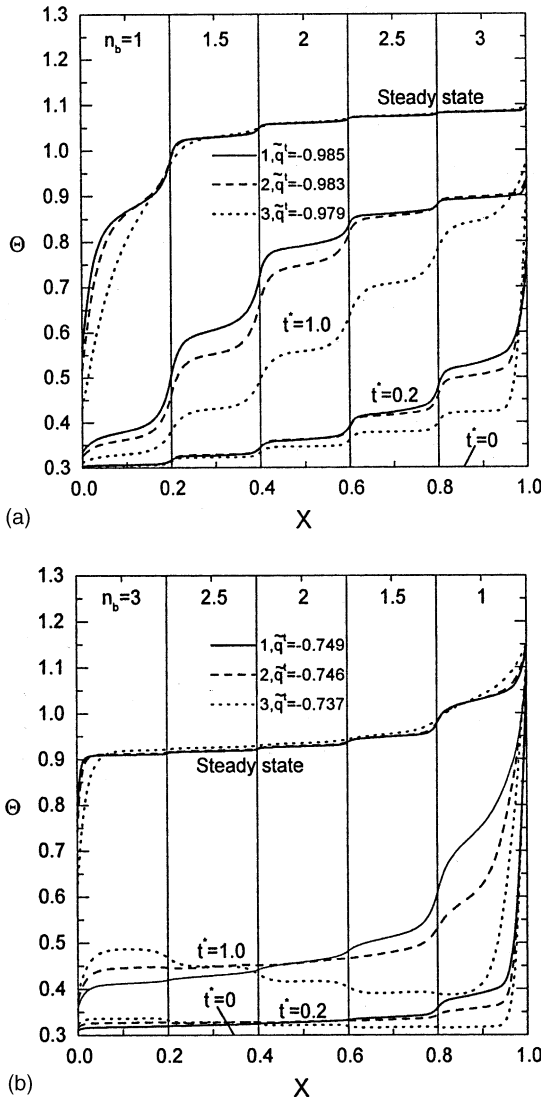

Fig. 7. Coupled heat transfer for radiative incidence on opaque surface. (a) Arranging refractive indexes increasingly along the thickness. (b) Arranging refractive indexes decreasingly along the thickness.

In short, from semitransparent surface to opaque surface direction, arranging refractive indexes increasingly has advantage for the composite transferring more heat.

4.3. Effect of layer thickness on coupled heat transfer

Keep the optical thickness ($\kappa_b L_b = 0.25$) and the other parameters of each layer in Fig. 6(a) unchanged, but change the thickness of each layer as $L_1 = 0.006$ m, $L_2 = L_4 = 0.005$ m, and $L_3 = L_5 = 0.002$ m. As shown in Fig. 8, the third layer have the biggest extinction coefficients due to its smallest thickness among all the layers, so that it can intensively absorb the radiative emitted by $S_{-\infty}$, and hence at the transient beginning a maximum temperature peak appears in the third layer. The fifth layer also has the biggest extinction coefficient, but the absorbing inside of opaque S_2 makes the highest temperature therein, so the maximum temperature peak does not appear in the fifth layer. The more intensively the medium of the composite scatters, the bigger the steady heat flux is.

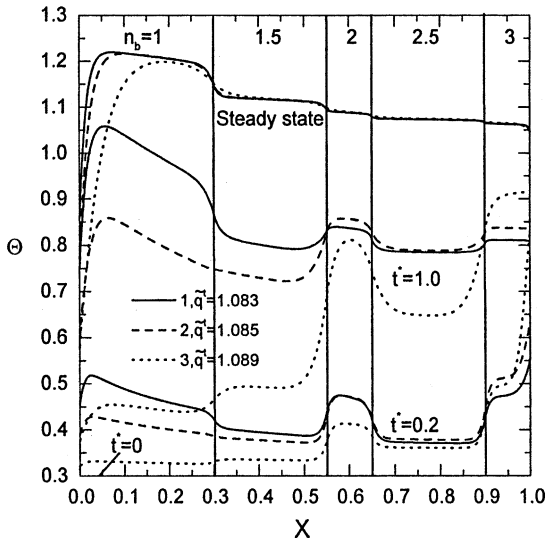

Fig. 8. Effect of layer thickness on coupled heat transfer.

4.4. Effect of refractive index on coupled heat transfer

The thickness of each layer in Fig. 9(a) is $L_b = 0.0025$ m, which is the half of that Fig. 6(a) and (b), the total thickness and total optical thickness is unchanged. The refractive index of each layer is indicated in the figure. Except for layer thickness and refractive index, the other parameters of each curve are the same with those of corresponding curve in Fig. 6(a) and (b). As shown, when the scattering albedo increases to $\omega_b = 0.9$, at the transient beginning the effect of total reflection at the interfaces apparently causes two maximum temperature peaks to be appeared the third and the eighth layer, respectively, which have critical angles to the layers on both sides of them due to their biggest refractive indexes. When the radiative energy emitted by $S_{-\infty}$ enters the composite from S_1, the scattered energy is totally reflected back if the incident angle of the scattered energy is greater than critical angle. Since the third and eighth layer are most intensively affected by the total reflection, the scattered energy absorbed by them is the most one and thus have the highest temperature. The increase in interfaces intensifies reflection and total reflection in the composite, and obstructs the radiative energy's transferring from the left to the right, so the steady heat flux is smaller than that of corresponding curve in Fig. 6(a) and (b). The increase in scattering albedo also causes the obstruction of the interfaces to radiative energy to increase, so the steady heat flux decreases.

As shown in Fig. 9(b), the layers of the composite have been increased to eighteen, the variation of refractive index along the thickness become more continuous, and the total thickness of the composite and other parameters are unchanged, the steady heat flux increases, and the temperature curves become smoother at the interfaces.

5. Conclusions

By the ray tracing method, the one-layer and multilayer radiative intensity quotient transfer model have been put forward here to trace the radiative intensity transferring in multilayer composite, and in combination with Hottel and Sarofim's zonal method and spectral band model, the RTCS have been deduced, and used to calculate the radiative heat source term. The following conclusions can be obtained:

(1) The increase in convective coefficients causes the steady heat flux to be increased.
(2) The emissivity of outside surface affects heat transfer in the composite more strongly than that of inside surface.
(3) The steady heat flux of radiative incidence on opaque surface is smaller than that of radiative incidence on semitransparent surface. From semitransparent surface directed to opaque surface, arranging refractive indexes increasingly has advantage for the composite transferring heat.
(4) For intensive scattering medium, the maximum temperature may appears in the layer with the biggest refractive index.
(5) If the variation of refractive index along the thickness direction becomes more continuous, the temperature curve becomes smoother and the heat flux increases.

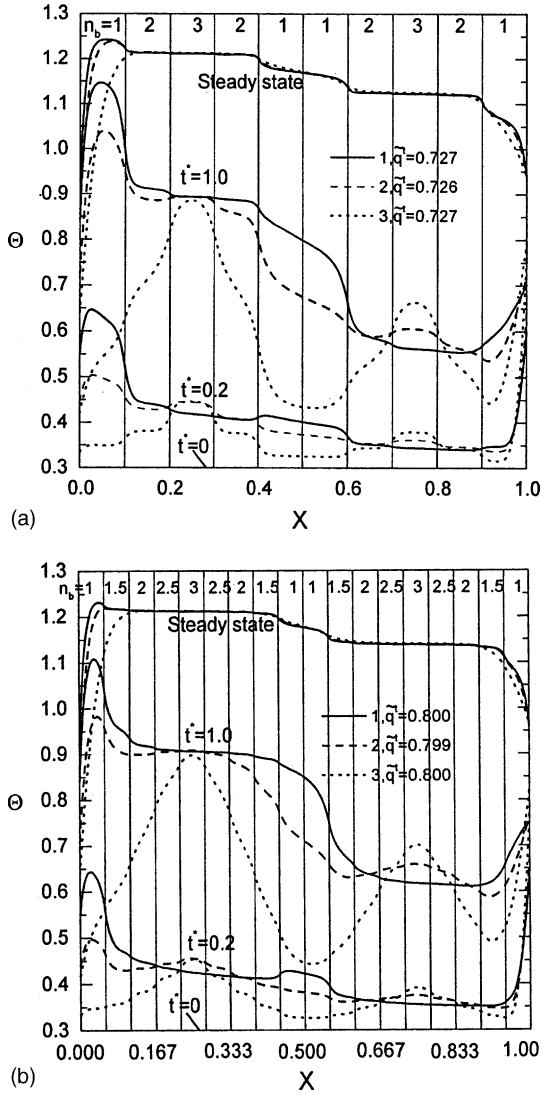

Fig. 9. Effect of refractive index on coupled heat transfer: (a) ten-layer composite and (b) eighteen-layer composite.

Acknowledgements

This research is supported by both the National Doctoral Foundation, from the Ministry of Education (MOE) and the National Natural Science Foundation of China (no. 59806003).

Appendix A. One-layer radiative intensity quotient transfer functions

The function that describes the radiative intensity transfer law in a single Semitransparent layer is defined as one-layer radiative intensity quotient transfer function, which is represented by symbol $\mathbf{F}^{a2_b}_{a1_b,k}$. Symbol $\mathbf{F}^{a2_b}_{a1_b,k}$ for the spectral radiative intensity received by superscript $a2_b$ to that emitted by subscript $a1_b$ at kth spectral band. Because the formulation form and the deducing process are the same no matter the medium is gray or non-gray, the subscript k is omitted below.

Let P_{b-1} and P_b be the two boundaries of the bth layer. The radiative intensity, emitted by the mth element (surface or control volume) at θ direction, enters the bth layer through P_{b-1} or P_b, will be reflected and attenuated repeatedly within

the layer until it finally becomes 0. By tracing this transfer process, the following expressions of the radiative intensity quotient transfer function are obtained.

$$\mathbf{F}_{P_{b-1'}}^{V_{I_b}} = \left\{\rho(\theta)_{b,b+1}\exp\left[-\kappa_b\left(L_b + x_{(I+1)_b}^{P_b}\right)\Big/\mu_b\right] + \exp\left(-\kappa_b x_{I_b}^{P_{b-1'}}/\mu_b\right)\right\}[1-\exp(-\kappa_b\Delta x_b/\mu_b)]/(1-\beta_1) \tag{A.1a}$$

$$\mathbf{F}_{P_b}^{V_{I_b}} = \left\{\rho(\theta)_{b,b-1}\exp\left[-\kappa_b\left(L_b + x_{I_b}^{P_{b-1'}}\right)\Big/\mu_b\right] + \exp\left(-\kappa_b x_{(I+1)_b}^{P_b}/\mu_b\right)\right\}[1-\exp(-\kappa_b\Delta x_b/\mu_b)]/(1-\beta_1) \tag{A.1b}$$

$$\mathbf{F}_{P_b}^{P_b} = \exp(-2\kappa_b L_b/\mu_b)\rho(\theta)_{b,b-1}/(1-\beta_1) \tag{A.1c}$$

$$\mathbf{F}_{P_{b-1'}}^{P_{b-1'}} = \exp(-2\kappa_b L_b/\mu_b)\rho(\theta)_{b,b+1}/(1-\beta_1) \tag{A.1d}$$

$$\mathbf{F}_{P_{b-1'}}^{P_b} = \mathbf{F}_{P_b}^{P_{b-1'}} = \exp(-\kappa_b L_b/\mu_b)/(1-\beta_1) \tag{A.1e}$$

$$\beta_1 = \exp(-2\kappa_b L_b/\mu_b)\rho(\theta)_{b,b-1}\rho(\theta)_{b,b+1} \tag{A.1f}$$

where $x_{(I+1)_b}^{P_b} = L_b - I\Delta x_b$, $x_{I_b}^{P_{b-1}} = (I-1)\Delta x_b$, and $\mu_b = \cos\theta_b$, where θ_b is the refractive angle of the bth layer. According to the Snell refractive law,

$$\theta_b = \arcsin(n_m \sin\theta/n_b) \tag{A.2}$$

where n_m is the refractive index of the mth element.

The radiative intensity emitted by the Ith control volume V_{I_b} is still reflected and attenuated repeatedly within the layer until it finally becomes 0. By tracing this process, the following expressions of the radiative intensity quotient transfer function are obtained.

$$\mathbf{F}_{V_{I_b}}^{P_b} = \mathbf{F}_{P_b}^{V_{I_b}} \tag{A.3a}$$

$$\mathbf{F}_{V_{I_b}}^{P_{b-1'}} = \mathbf{F}_{P_{b-1'}}^{V_{I_b}} \tag{A.3b}$$

$$\begin{aligned}\mathbf{F}_{V_{I_b}}^{V_{J_b}} = \Big\{&\exp\left(-\kappa_b x_{I_b}^{J_b}/\mu_b\right) + \rho(\theta)_{b,b-1}\exp\left[-\kappa_b\left(x_{I_b}^{P_{b-1'}} + x_{J_b}^{P_{b-1'}}\right)\Big/\mu_b\right] + \rho(\theta)_{b,b+1}\exp\left[-\kappa_b\left(x_{(I+1)_b}^{P_b} + x_{(J+1)_b}^{P_b}\right)\Big/\mu_b\right]\\ &+ \rho(\theta)_{b,b-1}\rho(\theta)_{b,b+1}\exp\left[-\kappa_b\left(2L_b - 2\Delta x_b - x_{V_{I_b}}^{V_{J_b}}\right)\Big/\mu_b\right]\Big\}[1-\exp(-\kappa_b\Delta x_b/\mu_b)]^2/(1-\beta_1)\end{aligned} \tag{A.3c}$$

$$\begin{aligned}\mathbf{F}_{V_{I_b}}^{V_{I_b}} = \Big\{&\rho(\theta)_{b,b-1}\exp\left(-2\kappa_b x_{I_b}^{P_{b-1'}}/\mu_b\right) + \rho(\theta)_{b,b+1}\exp\left(-2\kappa_b x_{(I+1)_b}^{P_b}/\mu_b\right)\\ &+ 2\rho(\theta)_{b,b-1}\rho(\theta)_{b,b+1}\exp\left[-\kappa_b\left(x_{I_b}^{P_{b-1'}} + L_b + x_{(I+1)_b}^{P_b}\right)\Big/\mu_b\right]\Big\}[1-\exp(-\kappa_b\Delta x_b/\mu_b)]^2/(1-\beta_1)\end{aligned} \tag{A.3d}$$

where $x_{I_b}^{J_b} = (|I-J|-1)\Delta x_b$, which is the distance between control volumes V_{I_b} and V_{J_b}.

In Eq. (A.3d), $\mathbf{F}_{V_{I_b}}^{V_{I_b}}$ denotes the quotient of the radiative intensity finally attenuated by V_{I_b} to that emitted by V_{I_b} after it passes through the boundaries I_b and $(I+1)_b$ of the control volume and transfers in the layer. But before the radiative energy, emitted by V_{I_b}, passes through the boundaries I_b and $(I+1)_b$, part of it that has been attenuated by the control volume itself can be expressed as $4\kappa_b\Delta x_b - 2[1-2E_3(\kappa_b\Delta x_b)]$. That is, it is necessary to add this term when calculating the RTC $(V_{I_b}V_{I_b})_{\mathrm{t-o},k}^{\mathrm{s}}$.

Furthermore P_0 and P_n will appear in Eqs. (A.1a)–(A.1f) and Eqs. (A.3a)–(A.3d) when calculating the first and the nth layer, and they need to be replaced by $S_1$and S_2 respectively.

Appendix B. Determination of reflectivity

The reflectivity $\rho(\theta)$ in Eqs. (A.1a)–(A.1f) and Eqs. (A.3a)–(A.3d) is a function of polarized component, so that each function $\mathbf{F}_{a1_b,k}^{a2_b}$ in Eqs. (A.1a)–(A.1f) and Eqs. (A.3a)–(A.3d) has a different value corresponding to the perpendicular and parallel components. For perfect dielectric medium, the effect of the extinction coefficient in the complex index of refraction can be neglected. When a radiative intensity transmits from the bth layer to its adjacent oth layer ($o = b-1$ or $b+1$), the reflectivity $\rho(\theta_b)_{bo}$ is

$$\rho_{\parallel}(\theta_b)_{bo} = [\tan(\theta_b - \varphi_o)/\tan(\theta_b + \varphi_o)]^2 \tag{B.1a}$$

$$\rho_{\perp}(\theta_b)_{bo} = [\sin(\theta_b - \varphi_o)/\sin(\theta_b + \varphi_o)]^2 \tag{B.1b}$$

where θ_b and φ_o are respectively the incident angle and the refractive angle respectively. According to Snell refractive law, the relationship between the two angles is

$$\varphi_o = \arcsin(n_b/n_o \sin\theta_b) \tag{B.2}$$

Substitute Eq. (A.2) into Eqs. (B.1a), (B.1b) and (B.2), then the reflectivity $\rho(\theta_b)_{bo}$, in Eqs. (B.1a) and (B.1b) can be written as $\rho(\theta)_{bo}$, which is only the function of angle θ. According to Eq.(A.2), When $n_b > n_o$ and $\theta_b > \arcsin(n_o/n_b)$, the total reflection occurs, then $\rho(\theta)_{bo} = 1$. That is, when an element emits a radiative intensity at angle θ, the reflectivity and total reflection at all the interfaces can be determined by the θ. When a radiative intensity transfers in the reverse direction without total reflection, the reflectivity is $\rho(\theta)_{ob} = \rho(\theta)_{bo}$, otherwise $\rho(\theta)_{ob} = 1$. If $n_b = n_o$, then $\rho(\theta)_{ob} = \rho(\theta)_{bo} = 0$. For opaque surface S_2, the reflectivity is determined by $\rho(\theta)_{ng} = 1 - \varepsilon_i$.

References

[1] R. Siegel, Transient thermal analysis of a translucent thermal barrier coating on a metal wall, ASME J. Heat Transfer 121 (1999) 478–481.

[2] R. Siegel, Radiative exchange in a parallel-plate enclosure with translucent protective coatings on it's walls, Int. J. Heat Mass Transfer 42 (1998) 73–84.

[3] S.H. Park, C.L. Tien, Radiation induced ignition of solid fuels, Int. J. Heat Mass Transfer 33 (1990) 1511–1520.

[4] S.S. Manohar, A.K. Kulkarni, S.T. Thynell, In-depth absorption of externally incident radiation in non-gray media, ASME J. Heat Transfer 117 (1995) 146–151.

[5] K.H. Lee, R. Viskanta, Comparison of the diffusion approximation and the discrete ordinates method for the investigation of heat transfer in glass, Glass Sci. Technol.: Glastechnische Berichte 72 (1999) 254–265.

[6] K.H. Lee, R. Viskanta, Transient conductive–radiative cooling of an optical quality glass disk, Int. J. Heat Mass Transfer 41 (14) (1998) 2083–2096.

[7] S. Svendsen, Solar collector with monolithic silica aerogel, J. Non-Cryst. Solids 145 (1992) 240–243.

[8] U. Heinemann, R. Caps, J. Fricke, Radiation–conduction interaction: an investigation on silica aerogels, Int. J. Heat Mass Transfer 39 (10) (1996) 2115–2130.

[9] R. Siegel, C.M. Spuckler, Effect of index of refraction on radiation characteristics in a heated absorbing, emitting, and scattering layer, ASME J. Heat Transfer 114 (1992) 781–784.

[10] R. Siegel, Effects of refractive index and diffuse or specular boundaries on a radiating isothermal layer, ASME J. Heat Transfer 116 (1994) 787–790.

[11] R. Siegel, C.M. Spuckler, Variable refractive index effects on radiation in semitransparent scattering multilayered regions, AIAA J. Thermophys. Heat Transfer 7 (1993) 624–630.

[12] R. Siegel, Refractive index effects on transient cooling of a semitransparent radiating layer, AIAA J. Thermophys. Heat Transfer 9 (1995) 55–62.

[13] C.C. Liu, R.L. Dougherty, Anisotropically scattering media having a reflective upper boundary, AIAA J. Thermophys. Heat Transfer 13 (2) (1999) 177–184.

[14] E.M. Abulwafa, Conductive–radiative heat transfer in an inhomogeneous slab with directional reflecting boundaries, J. Phys. D: Appl. Phys. 32 (1999) 1626–1632.

[15] M.H. Su, W.H. Sutton, Transient conductive and radiative heat transfer in a silica window, AIAA J. Thermophys. Heat Transfer 9 (2) (1995) 370–373.

[16] H.P. Tan, M. Lallemand, Transient radiative conductive heat transfer in flat glasses submitted to temperature, flux and mixed boundary conditions, Int. J. Heat Mass Transfer 32 (5) (1989) 795–810.

[17] H.P. Tan, J.F. Luo, X.L. Xia, Transient coupled radiation and conduction in a three-layer composite with semitransparent specular interfaces and surfaces, ASME J. Heat Transfer 124 (3) (2002) 470–481.

[18] J.F. Luo, X.L. Xia, H.P. Tan, T.W. Tong, Transient coupled heat transfer in three-layer composite with opaque specular surfaces, AIAA J. Thermophys. Heat Transfer 16 (3) (2002).

[19] J.F. Luo, H.P. Tan, L.M. Ruan, T.W. Tong, Refractive index effects on heat transfer in a multilayer composite with semitransparent surfaces, AIAA J. Thermophys. Heat Transfer, in press.

[20] H.P. Tan, J.F. Luo, L.M. Ruan, Q.Z. Yu, Transient coupled heat transfer in a multilayer composite with opaque specular surfaces and semitransparent specular interfaces, Int. J. Thermal Sci., in press.

[21] C.F. Tsai, G. Nixon, Transient temperature distribution of a multilayer composite wall with effects of internal thermal radiation and conduction, Numer. Heat Transfer 10 (1986) 95–101.

[22] V.P. Timoshenko, M.G. Trenev, A method for evaluating heat transfer in multilayered semitransparent materials, Heat Transfer-Soviet Res. 18 (5) (1986) 44–57.

[23] H.P. Tan, L.M. Rjuan, X.L. Xia, Q.Z. Yu, T.W. Tong, Transient coupled radiative and conductive heat transfer in an absorbing, emitting and scattering medium, Int. J. Heat Mass Transfer 42 (1999) 2967–2980.